Image Anal Stereol 2024;43:277-293 doi: 105566/ias.3037
Original Research Paper

A COMPLETED MULTI-SCALE LOCAL STATISTICS PATTERN FOR TEXTURE CLASSIFICATION

XIAOCHUN XU[1], BIN LI✉[, 2], Q.M. JONATHAN WU[3]
[1]Minjiang University, School of Computer and Big Data, Fuzhou, China, 350108; [2]Fujian Agriculture and Forestry University, College of Computer and Information Science, Fuzhou, China, 350002; [3]University of Windsor, 401 Sunset Avenue, Windsor, Canada, N9B3P4
e-mail: xuxiaochun0303@126.com; libin126email@126.com; jwu@uwindsor.ca
(Received September 23, 2023; revised June 22, 2024; accepted June 27, 2024)

ABSTRACT

Binary pattern methods play a vital role in extracting texture features. However, most of existing methods struggle to capture comprehensive and discriminative texture information. This paper aims to propose a novel multi-statistic binary pattern to extract rotation invariance statistic features for texture classification. First, this paper encodes the center pixel, mean, variance and range of local neighborhood by corresponding multi-scale threshold, and proposes the local center pattern, local mean pattern, local variance pattern and local range pattern. Then, based on the compact multi-pattern encoding strategy, the four sub-patterns are jointly encoded in a 4-bit binary pattern, named as multi-scale local statistics pattern. Finally, for comprehensive texture representation, the multi-scale local statistics pattern is jointly combined with local sign pattern and local magnitude pattern to generate a completed multi-scale local statistics pattern for texture classification. Extensive experiments conducted on three representative databases demonstrate that the proposed completed multi-scale local statistics pattern achieves competitive classification performance compared with other state-of-the-art approaches.

Keywords: feature extraction, local binary pattern, statistics encoding pattern, texture classification.

INTRODUCTION

Texture (Manjunath *et al.*, 2001; Wang *et al.*, 2019; Faust *et al.*, 2018) is the fundamental characteristic of an object surface, containing vital visual cues that enable computers to understand and analyze the appearance of an object. Texture classification plays a crucial role in digital image processing and pattern recognition, with diverse applications including as material classification (Liu *et al.*, 2015; Qi *et al.*, 2016), fingerprint recognition (Iloanusi and Ezema, 2017), remote sensing (Franklin, 2020; Patino and Duque, 2013; Van, 2012), and scene understanding (Lewicki, 2014; Kwak and Han, 2020). Due to the complex imaging environment, it is still a fundamental and challenging task to design a highly discriminative and efficient texture classification system.

Generally, texture can be defined as a property of the local spatial arrangement of pixel intensities in a local region. Over the past decades, numerous texture representation methods have been proposed to extract effective and efficient texture features. These methods can be categorized into five categories: statistical (Davis *et al.*, 1979), structural (Yu *et al.*, 2016), model-based (Cohen *et al.*, 1991), geometrical (Florindo and Bruno, 2013) and signal processing methods (Unser, 1995). Structural-based methods utilize the spatial arrangement attributes of textons to extract discriminative information, such as Laplacian of Gaussian (LoG) and Difference of Gaussian (DoG) methods. They are highly suitable for dealing with artificial regular textures, rather than complex and disordered natural textures. Model-based methods consider texture images as generative and stochastic models to achieve effective feature representation, such as Gaussian Markov Random Fields (GMFR) and multi-resolution autoregressive features. However, the computational requirements increase incrementally with the growing number of model parameters. Geometrical methods utilize geometric features to describe texture images, such as fractal geometry. For texture analysis, fractal dimension is used to measure the fractal geometry for the study of complex patterns in irregular texture images. Recently, researchers have combined fractal dimension with convolutional neural networks and achieve quite promising results (Florindo, 2024). The signal processing methods, also known as filter-based methods or transform methods, extract more descriptive texture information from the perspective of signal analysis, such as wavelet transform, Gabor filter, and filter banks. However, they are being confronted

with redundancy and performance bottleneck. Statistical methods (Kim and So, 2018; Cote and Albu, 2015; Bandzi *et al.*, 2007; Nguyen *et al.*, 2016; Pothos *et al.*, 2008; Varma and Zisserman, 2005) are one of the primary categories in texture classification, leveraging various statistical measurements of texture content to construct texture representations. The statistical texture representation is a long-lasting approach. Earlier statistical texture features focus on first-order, second-order, and higher-order statistics, such as the gray level difference matrix, gray-level co-occurrence matrix, and gray-level run-length matrix. Local statistical methods have well-established theoretical background and play a dominant role in resisting local texture variations caused by uncontrolled imaging conditions including illumination, rotation, scale and viewpoint changes. It has shown great potential for abstract and effective texture representation. However, the single statistical method fails to exploit the complementary and highly discriminative texture representation.

Combining different categories methods is a promising idea to address the above problem. The local binary pattern (LBP) (Ojala *et al.*, 2002a), a combination of statistical and structural method, is renowned for its efficiency and effectiveness to represent local texture. It achieves impressive discriminative power by encoding the sign of local difference between a center pixel and its neighbors. There are some advantages of LBP, including simple operation, dataset-independence, low complexity, and invariance to monotonic illumination changes. However, the traditional LBP only utilizes the sign of local difference, which is not sufficient to describe the various types of local texture information and is hard to deal with various complex imaging challenges. The scientific community has made significant efforts to improve and enhance the feature representation power of binary pattern methods.

In recent years, many LBP-based methods are proposed to enhance the texture representation power by exploiting diversified texture features. As one of the most famous LBP variants, the completed-LBP (CLBP) (Guo *et al.*, 2010a) stands out for its novel texture representation strategy. It not only considers the signs local differences but also introduces the magnitudes of local differences and the center pixels to enhance the local texture representation. In this way, it offers three sub-patterns (including CLBP_Sign, CLBP_Magnitude, and CLBP_Center) to represent texture images. Guo *et al.* (2010b) proposed the LBP variance (LBPV) by accumulating the local region variance into the LBP bins. Liu *et al.* (2012) proposed the extended local binary pattern (ELBP), which comprises two intensity-based sub-patterns (ELBP_CI- and ELBP_NI) and two difference-based sub-patterns (ELBP_RD and ELBP_AD). Later on, Li *et al.* (2016) introduced a median filter into the ELBP and proposed the median robust extended LBP (MRELBP), that demonstrated strong discriminative power and noise robustness. Recently, some works have been introduced that exploit various types of local differences to enhance local texture representation. Banerjee *et al.* (2018) found that the neighbors of a particular pixel hold significant amount of texture information and developed a local neighborhood intensity pattern (LNIP) by considering the relative local intensity difference for content-based image retrieval. Verma and Raman (2018) proposed a local neighborhood difference pattern (LNDP) by comparing the local neighbors mutually, and combined LNDP with the conventional LBP to generate the final feature vectors for natural and texture image retrieval. Pan *et al.* (2017) proposed the low dimensional feature-based LBP (FbLBP) by combining the sign of local difference with the mean and the variance of the magnitude. FbLBP is highly efficient to construct and does not require fine-tuning parameters. Zhang *et al.* (2017a) developed the normalized difference vector by taking advantage of the local difference and utilized the bag-of words to integrate the local features into a global image representation. To deal with complex imaging conditions, Wang *et al.* (2018) proposed a simple and effective jumping and refined local pattern. This method combines the jumping local difference count pattern with refined completed LBP, achieving notable effectiveness and providing scale, rotation, and illumination invariances. Song *et al.*, (2020) proposed the spatially weighted order binary pattern to exploit color order information for color texture classification, which not only extracts color order information for different channels but also represents the color order relationships in the spatial domain. A local neighborhood edge responsive binary pattern (LNERBP) (Ganesan and Santhanam, 2021) was developed to extract discriminative texture features from ocean bottom sediments. Additionally, the authors introduced a novel GMJAYA-ELM learning algorithms by integrating the extreme learning machine and Gaussian mutated JAYA. Furthermore, a local triangular coded pattern (LTCP) (Arya and Vimina, 2021) was presented by utilizing the horizontal and vertical relationship of local neighborhoods. It achieved satisfactory classification performance for texture and emotion classification tasks.

However, most LBP variants (Jain *et al.*, 2016; Liu *et al.*, 2019; Liu *et al.*, 2017) directly consider the intensity information of local neighborhood and ignore the statistical information of neighbors, such as mean, variance, and distribution. To address this limitation, some

binary pattern methods enhance the local texture description by taking advantage of statistical measures. For example, Nguyen *et al.* (2016) proposed statistical binary patterns based on a set of moment texture images to describe local contrast information and higher-order local variations. To achieve real-world texture classification, Cote and Albu (2015) presented a pixel-based local binary pattern statistics aggregation mechanism, achieving discriminative power and invariance against complex imaging conditions. Kim and So (2018) proposed directional statistical Gabor features based on different types of directional statistics from Gabor-filtered images, providing excellent classification performance on eight databases. Recently, with the assistance of statistical and combinatorial techniques, Silva and Florindo (2019) proposed a statistical descriptor based on the box counting fractal dimension to improve texture classification results. Despite the impressive results achieved by above methods, complex filtering and fractal processing lead to high computational cost.

To deal with this issue, this paper develops a new texture descriptor to extract informative and discriminative texture features by directly employing the statistical measures of neighbors, rather than utilizing filtered and fractal images. The main contributions of this paper are as follows:

First, this paper thoroughly leverages the statistical information of local neighborhoods and introduces three binary patterns with strict rotation invariance, including local mean pattern, local variance pattern, and local range pattern.

Then, this paper utilizes the multi-pattern encoding strategy to encode both the local center pattern and the aforementioned three binary patterns into a single 4-bit binary pattern, named as multi-scale local statistics pattern. It not only enriches the expressiveness of the center pattern but also provides more abstract texture information.

Finally, to achieve comprehensive texture representation, the multi-scale local statistics pattern is jointly combined with local sign pattern and local magnitude pattern to generate the completed multi-scale local statistics pattern for texture classification task.

Extensive experiments on three representative databases demonstrate that the propose completed multi-scale local statistics pattern achieves competitive even promising classification performance compared to other state-of-the-art approaches.

The rest of the paper is structured as follows. Section MATERIALS AND METHODS firstly reviews CLBP, then provides details on the proposed completed multi-scale local statistics pattern, and finally describes the distance measure. The experimental evaluations are presented in Section RESULTS. Finally, the analysis of the results and the conclusion are drawn in Section DISCUSSION.

MATERIALS AND METHODS

REVIEW OF CLBP

As one of the most successful variants of LBP, CLBP (Guo *et al.*, 2010a) captures texture information from three complementary components: the center pixel, the sign and magnitude of local difference. It then jointly encodes the corresponding sub-patterns, including CLBP_C, CLBP_S, and CLBP_M, to provide a more comprehensive texture representation. The essential operation of CLBP is as follows.

CLBP_S is equal to the original LBP, defined as:

$$CLBP\_S_{R,P} = \sum_{p=0}^{P-1} s\left(g_p - g_c\right)2^p, \tag{1}$$

where R is the sampling radius of the local neighborhood. g_c is the center pixel, and $g_p, p = 0,...,P-1$ are the corresponding neighborhood pixels. P is the number of neighbors. $s(\cdot)$ is the sign function, which can be formulated as:

$$s(x) = \begin{cases} 1, x \geq 0 \\ 0, x < 0 \end{cases}. \tag{2}$$

CLBP_M is obtained by encoding the local difference magnitude, with the threshold set as the mean of difference magnitudes for the whole image. Formally, CLBP_M is defined as:

$$CLBP\_M_{R,P} = \sum_{p=0}^{P-1} t\left(m_p, c_m\right)2^p, \tag{3}$$

where m_p represents the magnitude of local difference, described as:

$$m_p = \left|g_p - g_c\right|, \tag{4}$$

$t(\cdot)$ is the threshold function of binary encoding that is calculated as:

$$t(x,c) = \begin{cases} 1, x \geq c \\ 0, x < c \end{cases}, \tag{5}$$

c_m is the encoding threshold of m_p.

To achieve the rotation invariance, both CLBP_S and CLBP_M also utilize the rotation invariant uniform pattern (riu2) to construct the lookup table in histogram, which can be described as $CLBP\_S_{R,P}^{riu2}$ and $CLBP\_M_{R,P}^{riu2}$.

As an important complement of local difference, CLBP introduces CLBP_C to represent the texture information of center pixels. It is obtained using

$$CLBP\_C_{R,P} = t(g_c, c_I), \tag{6}$$

where c_I represents the encoding threshold of the center pixel, which is set as the average image intensity. $t(\cdot)$ is defined in formula (5).

To achieve the completed representation of local neighborhood, Guo *et al.* (2010a) jointly combined the three sub-patterns (including CLBP_S, CLBP_M and CLBP_C), described as CLBP_S/M/C.

CLBP entails some inherent issues. On one hand, it extracts the texture feature based on the original pixel gray value, which may overlook abstract and potential information in the neighborhood. Specifically, the three sub-patterns of CLBP are obtained by directly encoding the original pixel values. Intuitively, it would be more beneficial for feature representation to encode the binary pattern based on statistical measurements of pixels rather than original pixels. On the other hand, CLBP_C is only 1-bit, which could not effectively represent the texture image as an independent sub-pattern. Therefore, there are two issues that need to be resolved.

(1) How to effectively exploit potential texture information from local neighborhood.

(2) How to enhance CLBP_C to provide sufficient discriminative information for texture representation.

COMPLETED MULTI-SCALE LOCAL STATISTICS PATTERN

Multi-scale Local Statistics Pattern

To deal with the two issues concerning CLBP, this section develops a multi-scale local statistics pattern based on the statistical measures of the neighbors.

Given a center pixel g_c and its corresponding multi-scale threshold $thre_{N,g_c}$ according to literature (Xu *et al.*, 2020a), then the local center pattern (LCP) is defined as:

$$LCP_{R,P} = t\left(g_c, thre_{N,g_c}\right), \tag{7}$$

$$thre_{N,g_c} = \frac{1}{N}\sum_{k=1}^{N} lm_k(g_c). \tag{8}$$

The threshold function $t(\cdot)$ is defined in formula (5). $lm_k(g_c)$ is the local grid partitioning mean of g_c in scale k. $k \in [1, N]$ is hierarchical scale partitioning parameter and N is the number of scales.

The local mean pattern (LMP) measures the average level of neighbors, that can be calculated by:

$$LMP_{R,P} = t\left(m_{g_c,R,P}, thre_{N,m_{g_c,R,P}}\right), \tag{9}$$

where $m_{g_c,R,P}$ is the mean of P circular neighbors with radius R at g_c, defined as:

$$m_{g_c,R,P} = \frac{1}{P}\sum_{p=0}^{P-1} g_p, \tag{10}$$

$thre_{N,m_{g_c,R,P}}$ is the multi-scale threshold, computed as follows:

$$thre_{N,m_{g_c,R,P}} = \frac{1}{N}\sum_{k=1}^{N} lm_k\left(m_{g_c,R,P}\right). \tag{11}$$

$lm_k\left(m_{g_c,R,P}\right)$ is the local grid partitioning mean of $m_{g_c,R,P}$ in scale k.

The local variance reflects the intensity fluctuation of local neighborhood. Along this line, the local variance pattern (LVP) is proposed to exploit the intensity contrast information, which is defined as:

$$LVP_{R,P} = t\left(v_{g_c,R,P}, thre_{N,v_{g_c,R,P}}\right), \tag{12}$$

where $v_{g_c,R,P}$ is the variance of P circular neighbors with radius R at g_c, that is defined as:

$$v_{g_c,R,P} = \sum_{p=0}^{P-1}\left(g_p - m_{g_c,R,P}\right)^2 p\left(g_p\right), \tag{13}$$

$p(g_p)$ is the probability of g_p in the local neighborhood. The corresponding multi-scale threshold $thre_{N,v_{g_c,R,P}}$ is calculated by

$$thre_{N,v_{g_c,R,P}} = \frac{1}{N}\sum_{k=1}^{N} lm_k\left(v_{g_c,R,P}\right). \tag{14}$$

$lm_k\left(v_{g_c,R,P}\right)$ is the local grid partitioning mean of $v_{g_c,R,P}$ in scale k.

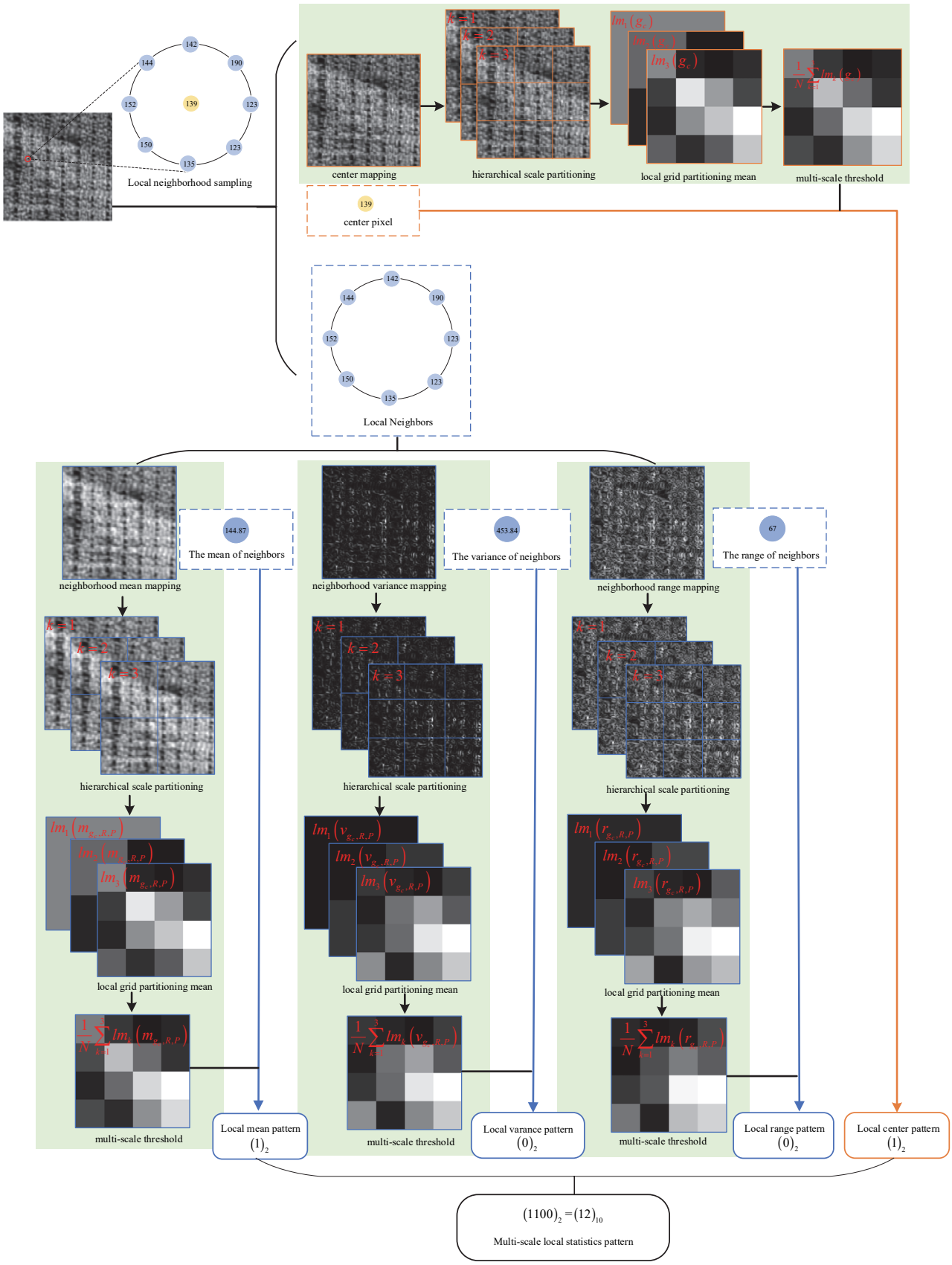

Fig. 1. *Illustration of the multi-scale local statistics pattern.*

The local range pattern (LRP) is computed by comparing the range of neighborhood pixels to the multi-scale threshold, which represents distribution of neighborhood intensity and can expressed as:

$$LRP_{R,P} = t\left(r_{g_c,R,P}, thre_{N,r_{g_c,R,P}}\right), \quad (15)$$

where $r_{g_c,R,P}$ is the range of P circular neighbors with radius R at g_c, defined as the difference between the maximum and minimum of the local neighborhood. The multi-scale threshold is represented as

$$thre_{N,r_{g_c,R,P}} = \frac{1}{N}\sum_{k=1}^{N} lm_k\left(r_{g_c,R,P}\right), \quad (16)$$

$lm_k\left(r_{g_c,R,P}\right)$ is the local grid partitioning mean of $r_{g_c,R,P}$ in scale k.

As shown in Fig. 1, there are four 1-bit sub-patterns derived from the local neighborhood statistics, including LCP, LMP, LVP, and LRP. However, an open question remains regarding how to combine these 1-bit sub-patterns to generate a compact and discriminative feature vector. Xu *et al.* (2021) proposed an MMC pattern that uses a compact multi-pattern encoding strategy to efficiently combine multiple 1-bit binary patterns.

In this paper, we employ the same strategy to fuse the proposed four sub-patterns to generate the multi-scale local statistics pattern (MLSP) for representing local texture statistical information. Formally, the local multi-scale statistics pattern is computed as

$$\begin{aligned} MLSP_{R,P} = {} & 2^0 \times LRP_{R,P} + 2^1 \times LVP_{R,P} \\ & + 2^2 \times LMP_{R,P} + 2^3 \times LCP_{R,P}. \end{aligned} \quad (17)$$

The multi-scale local statistics pattern compactly captures local statistical information, which can be advantageous, especially for handling complex intra-class variations. Moreover, the proposed multi-scale local statistics pattern exhibits three impressive properties:

(1) It is discriminative because it effectively encodes local texture statistical information.

(2) It provides satisfactory invariance to rotation, as the center pixel, mean, variance, and range of the local neighborhood remain unchanged regardless of image rotation.

(3) It has a compact form and high feature representation efficiency. Its feature dimensionality does not exponentially grow with the number of neighbors.

A Completed Multi-scale Local Statistics Pattern

In order to characterize the local texture information as comprehensively as possible, this paper divides the local texture region into three sub-features: the local statistical features, the sign feature of local difference, and the magnitude features of local difference. Then the three sub-features are encoded as three sub-patterns, the implementation is as follows.

Firstly, we design LCP, LMP, LVP, and LRP and propose MLSP based on the compact multi-pattern encoding strategy that effectively captures the statistics of the local texture region. Secondly, the local sign pattern (LSP) is designed to represent the sign of local difference, which is equal to the traditional LBP or CLBP_S. Thirdly, the local magnitude pattern (LMP) is encoded by the multi-scale threshold to capture the magnitude of local difference. Finally, we jointly combine MLSP, LSP, and LMP to generate the completed multi-scale local statistics pattern (CMLSP) for comprehensive local texture representation.

Fig. 2 illustrates the CMLSP descriptor. Specifically, the three sub-patterns of CMLSP are abbreviated as CMLSP_MS, CMLSP_LS, and CMLSP_MM, respectively. Now, we formulate the proposed completed multi-scale statistics pattern as follows.

CMLSP_MS is equal to MLSP described in Section Multi-scale Local Statistics Pattern that is represented as

$$\begin{aligned} CMLSP_{MS_{R,P}} = {} & 2^0 \times LRP_{R,P} + 2^1 \times LVP_{R,P} + \\ & 2^2 \times LMP_{R,P} + 2^3 \times LCP_{R,P}. \end{aligned} \quad (18)$$

CMLSP_LS is equal to CLBP_S, which is described as

$$CMLSP\_LS_{R,P} = \sum_{p=0}^{P-1} s\left(g_p - g_c\right)2^p. \quad (19)$$

CMLSP_MM characterizes the magnitude information of local difference. To achieve efficient multi-scale representation, CMLSP_MM is designed based on the multi-scale threshold of magnitude components that can be calculated as

$$CMLSP\_MM_{R,P} = \sum_{p=0}^{P-1} t\left(m_p, thre_{N,m_p}\right)2^p, \quad (20)$$

where $thre_{N,m_p}$ is the multi-scale threshold of m_p that is represented as

$$thre_{N,m_p} = \frac{1}{N}\sum_{k=1}^{N} lm_k\left(m_p\right). \quad (21)$$

$lm_k\left(m_p\right)$ is the local grid partitioning mean of m_p in scale k.

It needs to be noted that CMLSP_LS adopts the center pixel to encode the sign information instead of using multiscale thresholding. In the texture analysis community, the general consensus is that microstructural texture information holds greater significance than macrostructural details. For a more comprehensive representation, CMLSP_LS utilizes pixel-level thresholds to capture micro-texture, whereas CMLSP_MS and CMLSP MM employ multi-scale thresholds to represent macro-texture.

Finally, the three sub-patterns (including CMLSP_MS, CMLSP_LS, and CMLSP_MM) are jointly fused to generate the completed local texture representation, denoted as CMLSP_LS/MM/MS. For simplicity, the fusion feature CMLSP_LS/MM/MS is abbreviated as CMLSP in the subsequent descriptions.

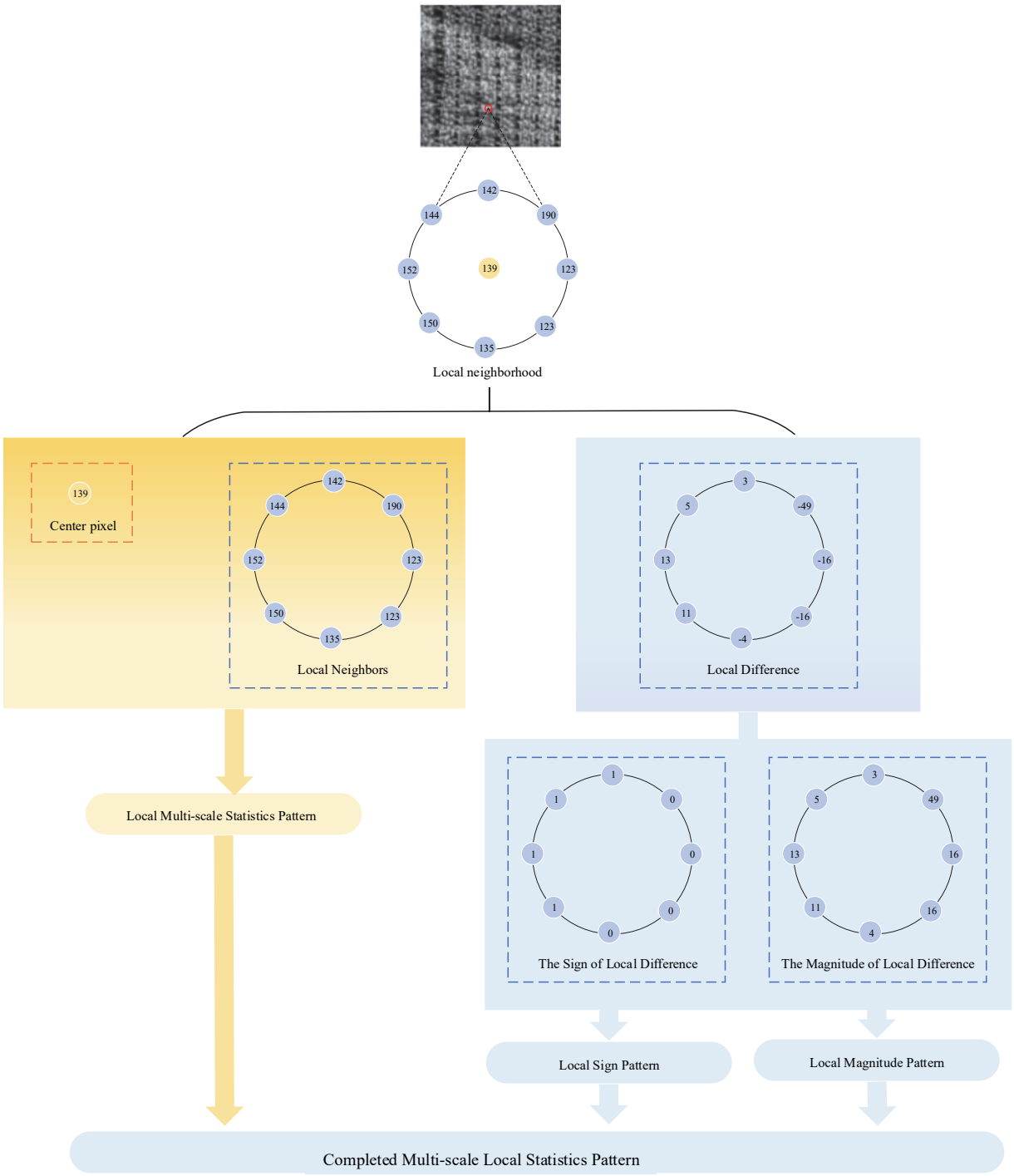

Fig. 2. *Illustration of the completed multi-scale local statistics pattern.*

DISTANCE MEASURE

For a fair comparison, the proposed texture descriptor and competitors adopt the same classifier for experimental evaluation. More especially, this paper uses the nonparametric nearest neighbor classifier with χ^2 distance to measure the dissimilarities between training images and sample images.

The histograms of the sample image and the training image are described as H^S and H^T, respectively. Then the χ^2 distance is defined as

$$D\left(H^S, H^T\right) = \sum_{i=1}^{M} \frac{\left(H_i^S - H_i^T\right)^2}{H_i^S + H_i^T}, \quad (22)$$

where M is the total number of bins. And i refers to the $i-th$ bin in the corresponding histogram.

RESULTS

To validate the superiority of the proposed CMLSP_LS/MM/MS descriptor for the texture classification task, we conduct a series of comprehensive experimental evaluations, including comparisons with state-of-the-art descriptors, on several well-known texture classification databases such as Outex (Ojala *et al.*, 2002b), UMD (Xu *et al.*, 2006), and UIUC (Dana *et al.*, 1999).

CLASSIFICATION BENCHMARK AND IMPLEMENTATION DETAILS

The Outex database (Ojala *et al.*, 2002b) is a popular texture benchmark captured under various imaging conditions, including nine rotation angles and three illuminations. We evaluate rotation invariance using Outex_TC10 and analyze illumination and rotation invariance using Outex_TC12 (including Outex_TC12_000 and Outex_TC12_001). More especially, Outex_TC10 contains 24 texture classes, each containing 180 texture images with dimensions of 128*128. There are 480 (24*20) images for training, and the rest 3840 (24*160) images are used for testing. Outex_TC12 contains 24 texture classes with a total of 9120 images captured under nine rotation angles (00, 50, 100, 150, 300, 450, 600, 750, and 900) and three illuminations (inca, t184, and horizon). The training set contains texture images with the rotation angle of 0o and inca illumination condition, while the test set comprises images with varying rotation angles and illumination conditions.

The UMD database (Xu *et al.*, 2006) contains 1000 real-world texture images with dimensions of 1280*960, collected under various viewing angles, illuminations, and spatial resolutions. It consists of 25 texture classes, with each class containing 40 texture images. Following the standard evaluation protocol, we randomly select 20 samples for the training set, with the remainder used for testing. This random partitioning is independently implemented 50 times, and the mean of the results is regarded as the final classification outcome.

The UIUC database (Dana *et al.*, 1999) is a publicly available and challenging texture database consisting of 25 texture classes. Each class contains 40 samples with dimensions of 640*480, captured under various rotations, scales, viewpoints, and resolutions. For the experimental evaluation, half of the texture images are randomly selected for training, and the remaining half is considered as the testing set. Similar to UMD, we use the average accuracy over 50 independent partitions as the final classification result.

Details of the three texture databases are presented in Table 1. Fig. 3 shows some texture samples from the Outex, UMD, and UIUC database.

EXPERIMENTAL EVALUATION IN OUTEX DATABASE

To visualize the performance improvements of the proposed CMLSP compared to the baseline CLBP, Fig. 4 shows the classification accuracies on the Outex_TC10 dataset with different sampling resolutions.

Table 1. *Details of three texture classification databases.*

Database	Num. of images	Num. of classes	Size	Experimental Evaluation
Outex_TC10	4830	24	128*128	Rotation invariance
Outex_TC12	9120	24	128*128	Illumination and rotation invariance
UMD	1000	25	1280*960	Robustness of complex imaging conditions
UIUC	1000	25	640*480	Robustness of complex imaging conditions

It is observed that the introduction of local statistical features (represented as CMLSP_MS) significantly and consistently boosts the classification performance. For example, with (R, P) = (3, 24), the CMLSP_LS/MS achieves an accuracy of 99.84%, which is higher than that of CLBP_S/C (97.97%). With the same sampling resolution, CMLSP_MM/MS also produces a performance improvement of 1.07 percentage points (p.p.) compared with CLBP_M/C. The fusion feature CMLSP_LS/MM/MS achieves the highest classification accuracy of 99.95%, surpassing the baseline CLBP_S/M/C. This highlights the superior discriminability of CMLSP_MS compared to traditional CLBP_C. Similar conclusions can be drawn for other sampling resolutions. Besides, Table 2 reports the feature dimension of the proposed CMLSP and CLBP. As we can see, the excellent classification performance of our CMLSP comes at the cost of some computational overhead. However, its feature dimension does not experience exponential growth. Hence, the proposed CMLSP provides valuable insights into achieving a balance between performance and feature dimension.

To further verify the effectiveness of the proposed CMLSP, we compare it with some state-of-the-art methods on Outex_TC10 and Outex_TC12. As shown in Table 3, the proposed CMLSP descriptor demonstrates remarkable discriminative power for the texture classification task. For instance, on TC10, CMLSP reaches the highest accuracy of 99.95% with (R, P) = (3, 24). With the same sampling resolution, it also achieves the best classification rate of 98.66% and 98.63% on TC12_000 and TC12_001, respectively.

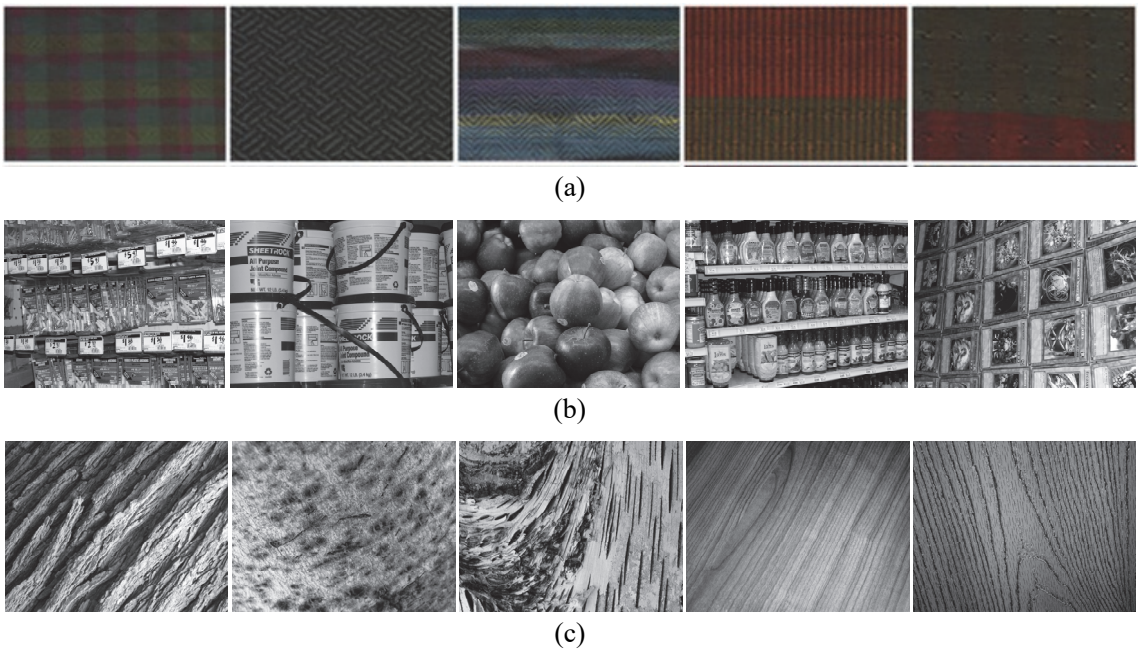

Fig. 3 *Some texture samples of (a) Outex database, (b) UMD database, and (c) UIUC database.*

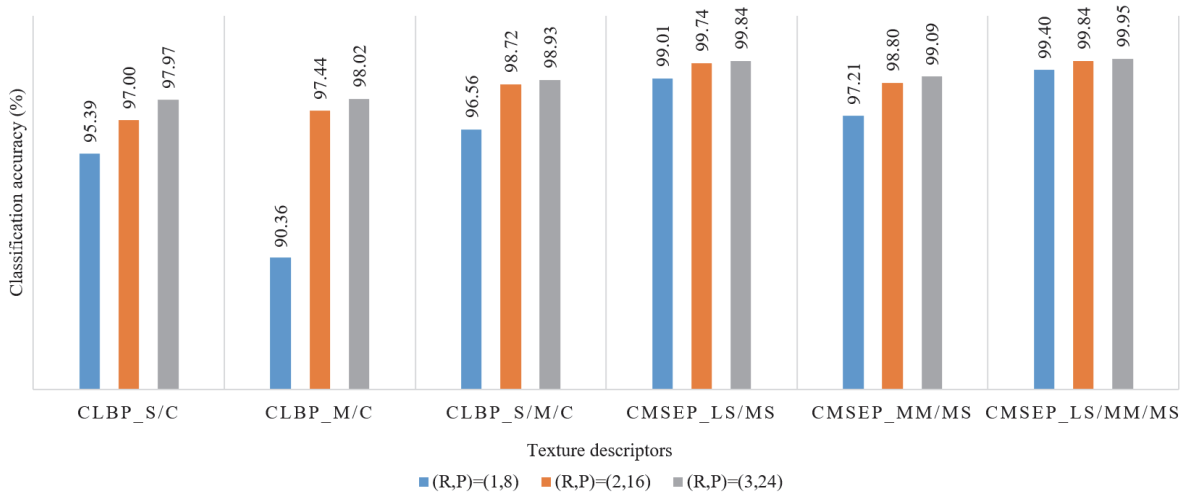

Fig. 4 *Classification accuracy on Outex_TC10 of the proposed CMLSP and CLBP.*

Table 2 *Feature dimension of the proposed CMLSP and CLBP.*

(R, P)	(1, 8)	(2, 16)	(3, 24)
CLBP_S/C	20	36	52
CLBP_M/C	20	36	52
CLBP_S/M/C	200	648	1352
CLBP_LS/MS	160	288	416
CLBP_MM/MS	100	324	676
CMLSP_LS/MM/MS	1600	5184	10816

Table 3. *Classification accuracy (%) of CMLSP and state-of-the-art descriptors on the Outex database.*

(R, P)	(1, 8)			(2, 16)			(3, 24)		
Method	Outex_TC10	Outex_TC12		Outex_TC10	Outex_TC12		Outex_TC10	Outex_TC12	
		000	001		000	001		000	001
LBP (Ojala *et al.*, 2002a)	84.81	65.46	63.68	89.40	82.26	75.20	95.07	85.04	80.78
CLBP_S/M/C (Guo *et al.*, 2010a)	96.56	90.30	92.29	98.72	93.54	93.91	98.93	95.32	94.53
CLBC (Zhao *et al.*, 2012)	97.16	89.79	92.92	98.54	93.26	94.07	98.78	94.00	93.24
LTP (Tan and Triggs, 2010)	94.56	72.25	71.83	96.09	88.26	86.26	97.83	93.38	89.26
CRLBP ($_{\alpha = 8}$)(Zhao *et al.*, 2013)	97.55	91.94	92.45	98.59	95.88	96.41	99.35	96.83	96.16
CRLBP ($_{\alpha = 1}$)(Zhao *et al.*, 2013)	96.54	91.16	92.06	98.85	96.67	96.97	99.48	97.57	97.34
BRINT (Liu *et al.*, 2014)	91.87	86.46	88.50	96.43	93.38	93.98	96.04	94.24	94.35
SCLBP TC (t = 3) (Nguyen *et al.*, 2014)	98.25	92.45	94.25	99.36	95.05	96.47	99.45	96.68	98.25
$CRDP_{3D}$_2 (Wang *et al.*, 2017)	97.03	92.69	94.81	98.33	96.41	94.95	98.52	95.46	91.44
AECLBP_S/M/C (Song *et al.*, 2015)	97.58	91.83	91.81	98.80	95.42	94.70	99.19	96.83	95.05
$DRLBP_3$ (Mehta and Egiazarian, 2016)	88.54	84.25	83.19	99.19	97.15	95.37	-	-	-
CDLF_S/M/C (Zhang *et al.*, 2017b)	97.29	91.06	93.31	99.48	94.24	95.02	99.11	95.65	95.25
CDLF_S/M/C_AHA (Zhang *et al.*, 2017b)	97.45	91.62	94.03	99.64	94.40	95.44	99.22	96.02	95.67
FbLBP (Pan *et al.*, 2017)	98.85	92.66	93.82	99.64	95.42	95.69	99.58	96.00	94.75
CRMCLBP (Li *et al.*, 2018)	98.05	92.71	94.33	99.04	96.88	97.55	99.32	97.89	97.89
CLEBP (Xu *et al.*, 2020a)	**99.58**	94.79	94.93	99.74	**98.17**	97.62	99.87	98.03	97.92
CLSP (Xu *et al.*, 2020b)	98.93	**94.91**	94.81	99.58	98.10	96.90	99.40	98.31	97.31
CMLSP_LS/MM/MS	99.40	94.79	**95.46**	**99.84**	97.15	**98.10**	**99.95**	**98.66**	**98.63**

On TC10, compared with the baseline CLBP, the proposed CMLSP descriptor achieves improvements of 2.84 p.p., 1.12 p.p., and 1.02 p.p. in the case of (R, P) = (1, 8), (2,16), and (3, 24), respectively. It also outperforms other CLBP variants in classification performance. For instance, CMLSP reaches the best accuracy of 99.95% with (R, P) = (3, 24), surpassing CLBC, CRLBP, SCLBP_TC, and AECLBP by 1.17 p.p., 0.47 p.p., 0.50 p.p., and 0.76 p.p., respectively. In addition, CMLSP performs slightly better than some recent texture descriptors. More precisely, it demonstrates improvements of 0.37 p.p., 0.63 p.p., 0.08 p.p., and 0.55 p.p. over FbLBP, CRMCLBP, CLEBP, and CLSP, respectively. Its superior performance on TC10 validates the powerful rotation invariance of CMLSP_MS. The main reason is that regardless of rotation changes, the local statistics remain consistent.

On TC12_000 and TC12_001, CMLSP also exhibits impressive classification performance. For instance, on TC12_000, the proposed CMLSP descriptor outperforms the baseline CLBP by a significant margin, with a 3.34 p.p. improvement. Additionally, it maintains superiority over CRLBP by 1.09 p.p., AECLBP by 1.83 p.p., and CDLF by 2.64 p.p., respectively. Compared with recent texture classification methods, CMLSP outperforms FbLBP, CRMCLBP, CLEBP, and CLSP by 2.66 p.p., 0.77 p.p., 0.63 p.p., and 0.35 p.p., respectively. To further verify its effectiveness in handling illumination variance, we conduct experimental evaluations on TC12_001. Similar to TC12_000, the proposed CMLSP still gains significant performance improvements compared to its competitors. The superior performance improvement is mainly attributed to the powerful complementary and highly discriminative information extracted by the proposed CMLSP_LS/MM/MS.

EXPERIMENTAL EVALUATION IN UMD DATABASE

To better illustrate the classification performance of different sub-patterns and fusion features from the proposed CMLSP descriptor, Fig. 5 shows their classification accuracies for varying numbers of training images (20, 15, 10, and 5) with (R, P) = (3, 24) on the UMD database.

As can be seen, firstly, the classification accuracies increase with the number of training images and peak at 20 training samples. Secondly, among different sub-patterns, the proposed CMLSP_MS achieves the highest classification accuracy of 93.98% with 20 training images, indicating its superior informativeness and discriminative power. Thirdly, the fusion feature CMLSP_LS/MM/MS achieves the best classification accuracy of 98.89% with 20 training images, followed by CMLSP_LS/MS (98.66%) and CMLSP_MM/MS (98.24%). This confirms the effectiveness of multi-pattern fusion in enhancing classification performance. Based on the results of the observational experiment shown in Fig. 5, it is evident that the proposed CMLSP_MS offers promising, valuable, and discriminative information for comprehensive texture representation.

To further highlight the classification performance of the proposed CMLSP descriptor, some classical and state-of-the-art descriptors are adopted as competitors in Table 4. For a fair comparison, we conduct the same data split strategy with competitors in Table 4. Besides, we report metric values as shared by the original authors to make the experimental comparison results more convincing.

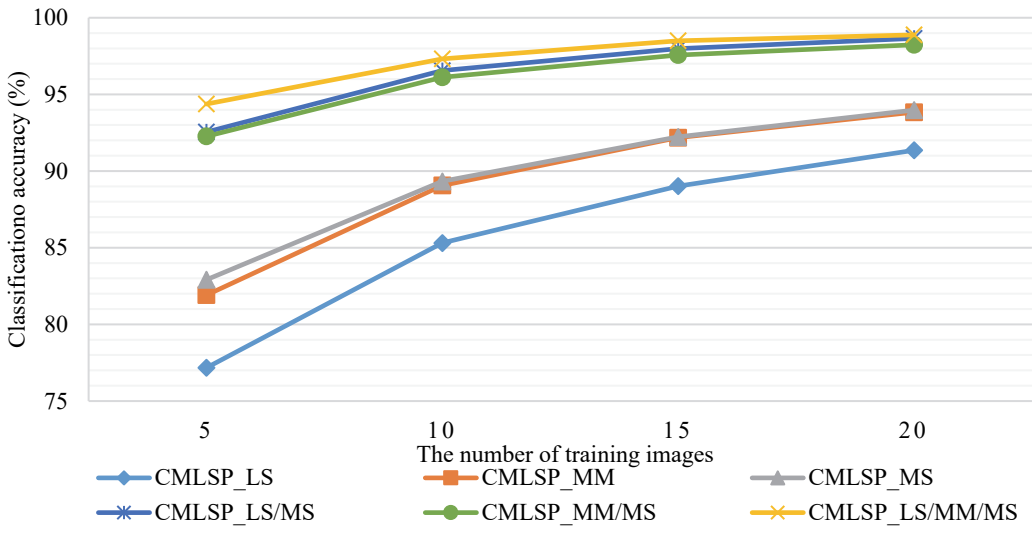

Fig. 5. *Classification accuracy for varying numbers of training images on the UMD database.*

As shown in Table 4, the proposed CMLSP_LS/MM/MS descriptor reaches the highest accuracy with 20 training images for (R, P) = (3, 24). Additionally, several interesting conclusions can be drawn.

Firstly, compared with the baseline CLBP, the proposed CMLSP_LS/MM/MS achieves significant improvements of 6.02 p.p., 6.36 p.p., 6.85 p.p., and 6.83 p.p. over CLBP with 20, 15, 10, and 5 training images, respectively, in the case of (R, P) = (3, 24). In addition, it also achieves improvements of 12.64 p.p., 14.51 p.p., 16.86 p.p., and 22.13 p.p. over traditional LBP under the same experimental conditions. Secondly, CMLSP_LS/MM/MS outperforms other classical LBP variants. For example, its best result surpasses the best results of LTP, BRINT, MRELBP, and CRDP by 8.46 p.p., 5.93 p.p., 4.59 p.p., and 6.79 p.p., respectively, with 20 training images in the case of (R, P) = (3, 24). Thirdly, compared with some recent texture descriptors, CMLSP_ LS/MM/MS obtains remarkable classification performance on the UMD database. More significantly, we note that the best result of CMLSP_LS/MM/MS is higher than AELTP and AECLBP by 4.72 p.p. and 2.03 p.p., respectively. It also outperforms CRDPCPS and CLBPCPS by 5.57 p.p. and 5.39 p.p., respectively.

Table 4. *Classification accuracy (%) of CMLSP and state-of-the-art methods on the UMD database*

Methods	(R, P)	The number of training examples			
		20	15	10	5
LBP (Ojala *et al.*, 2002a)	(1, 8)	84.09	81.80	77.89	70.28
	(2, 16)	84.67	82.28	7873	70.81
	(3, 24)	86.25	83.99	80.47	72.25
LTP (Tan and Triggs, 2010)	(1, 8)	84.24	82.48	79.14	71.71
	(2, 16)	87.73	86.33	83.43	76.45
	(3, 24)	89.30	87.37	84.75	77.57
	(5, 24)	90.43	89.08	85.78	78.81
AELTP (Song *et al.*, 2015)	(1,8)	89.10	86.06	82.59	73.46
	(2,16)	91.94	91.24	86.84	80.71
	(3,24)	94.17	91.58	88.91	80.43
BRINT (Liu *et al.*, 2014)	(2, 8)	91.87	90.92	89.38	84.91
	(3, 8)	92.34	90.74	90.10	85.42
	(5, 8)	92.96	91.92	90.32	84.63
MRELBP (Liu *et al.*, 2016)	(2, 8)	93.58	92.72	91.36	88.10
	(3, 8)	94.30	93.85	92.87	89.31
	(5, 8)	94.15	93.85	92.06	87.29
CRDP (Wang *et al.*, 2017)	(1, 8)	91.82	90.93	89.45	85.15
	(2, 16)	91.91	91.13	89.52	84.79
	(3, 24)	92.10	91.16	89.24	84.11
	(5, 24)	92.06	91.05	88.87	83.26
$CRDP_{CPS}$ (Pan *et al.*, 2019)	-	93.32	92.84	91.41	87.67
CLBP (Guo *et al.*, 2010a)	(1, 8)	92.16	91.56	90.31	86.95
	(2, 16)	92.82	92.16	90.62	87.04
	(3, 24)	92.87	92.14	90.48	87.55
AECLBP (Song *et al.*, 2015)	(1,8)	96.48	95.84	93.63	90.99
	(2,16)	96.86	95.71	95.05	91.42
	(3,24)	96.78	96.80	94.47	91.79
$CLBP_{CPS}$ (Pan *et al.*, 2019)	-	93.50	92.87	91.35	88.31
CLSP (Xu *et al.*, 2020b)	-	98.49	97.24	96.39	92.00
CMPE (Xu *et al.*, 2021)	(2, 8)	98.47	97.67	96.47	92.82
	(3, 16)	98.75	98.20	96.94	93.32
	(3, 24)	98.84	98.12	97.03	93.26
	(5, 24)	98.78	98.20	96.91	93.05
CMLSP_LS/MM/MS	(1,8)	98.17	97.41	96.07	92.79
	(2,16)	98.78	98.41	97.25	94.09
	(3,24)	**98.89**	**98.50**	**97.33**	**94.38**

Moreover, CMLSP_LS/MM/MS slightly outperforms the recently reported CMPE, and provides a 0.4 p.p. performance increase compared to the CLSP descriptor. Fourthly, it is noticed that our CMLSP_LS/MM/MS descriptor performs favorably with corresponding to small training samples. CMLSP_LS/MM/MS achieves the highest classification score of 94.38% with 5 training images in the case of (R, P) = (3, 24). The performance improvement over LBP and CLBP is 22.13 p.p. and 6.83 p.p. under the same experimental conditions. Furthermore, the best result of CMLSP_LS/MM/MS also achieves significant improvements of 15.57 p.p., 8.96 p.p., 5.07 p.p., and 9.15 p.p. over LTP, BRINT, MRELBP, and CRDP, respectively. Additionally, the proposed CMLSP_LS/MM/MS also yields better results than recently proposed CLSP and CMPE.

To sum up, CLMSP_LS/MM/MS descriptor not only impressively outperforms the performance of classical binary pattern descriptors but also performs favorably against state-of-the-art texture descriptors. Its striking performance comes from the introduction of CMLSP_MS, which is confirmed by the fact that CMLSP_MS performs better than CMLSP_LS and CMLSP_ MM in Fig. 5, and the fusion feature CMLSP_LS/MM/MS achieves the best classification result in Table 4.

EXPERIMENTAL EVALUATION IN UIUC DATABASE

The UIUC database serves as a challenging and representative benchmark for the texture classification task, containing various difficult imaging conditions including arbitrary rotations, significant viewpoint and scale variations, and uncontrolled illumination conditions. To further verity the effectiveness of the proposed CMLSP_LS/MM/MS descriptor, we compare it with some classical and state-of-the-art texture classification methods in Table 5. A number of significant observations from Table 5 are as follows.

Table 5. *Classification accuracy (%) of CMLSP and state-of-the-art descriptors on the UIUC database*.

Methods	(R, P) = (1, 8)				(R, P) = (2, 16)				(R, P) = (3, 24)			
	20	15	10	5	20	15	10	5	20	15	10	5
LBP (Ojala *et al.*, 2002a)	54.65	52.94	47.14	39.72	61.32	56.42	51.16	42.67	64.05	60.05	54.25	44.59
LTP (Tan and Triggs, 2010)	68.56	65.21	60.34	51.21	78.50	75.45	69.96	59.46	82.28	78.48	73.19	61.84
CLBP (Guo *et al.*, 2010a)	87.64	85.70	82.65	75.05	91.04	89.42	86.29	78.57	91.19	89.21	85.95	78.05
CLBC (Zhao *et al.*, 2012)	87.83	85.66	82.35	74.57	91.04	89.66	86.63	79.48	91.39	90.10	86.45	79.75
CRLBP ($\alpha = 8$)(Zhao *et al.*, 2013)	88.08	86.62	82.97	76.01	91.99	90.41	88.04	81.49	92.83	90.55	88.02	80.54
CRLBP ($\alpha = 1$)(Zhao *et al.*, 2013)	86.91	85.67	82.20	73.95	92.92	91.82	88.15	81.98	93.31	92.03	89.47	81.90
BRINT (Liu *et al.*, 2014)	79.52	76.14	71.26	61.59	84.14	81.57	77.06	67.96	86.39	83.77	79.33	70.34
AECLBP (Song *et al.*, 2015)	88.04	86.54	82.96	75.43	90.68	89.18	85.17	78.13	92.18	90.22	87.08	79.69
LVQP (Pan *et al.*, 2015)	88.08	85.55	81.81	73.30	93.45	91.96	89.03	81.85	94.79	93.42	90.70	84.12
CRDP (Wang *et al.*, 2017)	84.39	81.69	77.28	68.42	89.48	86.94	83.04	73.02	89.69	87.44	83.05	73.66
LQC_C(2)N(4) (Zhao *et al.* 2016)	89.45	87.70	83.58	76.23	92.32	90.58	87.67	81.48	92.94	90.39	87.54	81.64
LQC_C(6)N(4) (Zhao *et al.* 2016)	90.12	88.54	85.62	78.38	92.62	90.76	87.97	81.98	93.17	90.91	88.13	81.77
CDLF_S/M/C (Zhang *et al.* 2017b)	89.57	87.73	84.74	78.39	92.85	90.17	88.73	80.55	92.90	91.18	87.34	81.78
CDLF_S/M/C_AHA (Zhang *et al.* 2017b)	90.16	88.30	85.17	78.82	94.10	90.53	89.58	80.82	93.77	92.83	88.80	82.11
EMCLBP (Shakoor and Boostani, 2017)	87.92	84.37	83.30	75.30	92.19	90.59	87.72	80.46	92.99	91.29	88.11	80.47
FbLBP (Pan *et al.*, 2017)	92.04	90.27	87.80	80.10	94.14	92.73	89.79	82.43	94.17	92.58	89.51	81.79
$FbLBP_{ACPS}$ (Pan *et al.*, 2021)	92.54	90.89	87.96	80.60	94.34	93.20	90.63	83.33	94.74	93.24	90.24	82.52
CLEBP (Xu *et al.*, 2020a)	**93.54**	**91.65**	**89.01**	**82.29**	95.54	93.98	91.35	84.75	**96.40**	94.96	92.67	86.36
CMPE (Xu *et al.* 2021)	91.43	89.40	85.95	78.02	94.97	93.56	90.52	83.26	94.89	93.52	90.18	82.73
CMLSP_LS/MM/MS	91.97	90.30	86.83	80.35	**95.58**	**94.65**	**92.70**	**86.52**	96.28	**95.22**	**92.90**	**86.50**

First of all, the proposed CMLSP_LS/MM/MS descriptor achieves the best classification accuracy with different numbers of training samples in the case of (R, P) = (3, 24), demonstrating its superiority over other descriptors in Table 5. Secondly, the best result of CMLSP_LS/MM/MS significantly outperforms the best results of classical LBP, LTP, and BRINT by 32.23 p.p., 14.00 p.p., and 9.89 p.p., respectively. Additionally, it surpasses the best result of basic CLBP by 5.09 p.p. The key reason for this performance superiority lies in two factors. The first factor is that the proposed sub-pattern CMLSP_MS considers rich statistical information, which is very informative for texture representation. The second factor is that the fusion feature CMLSP_LS/MM/MS enhances the classification accuracy by providing strongly complementary and highly discriminative texture information. Thirdly, the proposed CMLSP_LS/MM/MS achieves significant performance improvement when compared with some successful CLBP variants. For example, it achieves improvements of 4.89 p.p., 5.12 p.p., 6.45 p.p., and 6.75 p.p. over CLBC corresponding to 20, 15, 10, and 5 training images, respectively. Moreover, it also surpasses the best results of CRLBP (α=1), AECLBP, Z CDLF_S/M/C_AHA, and EMCLBP by 2.97 p.p., 4.10 p.p., 2.51 p.p., and 3.29 p.p., respectively. It confirms that the proposed sub-pattern CMLSP_MS efficiently enhances the classification performance. Fourthly, compared with some recently proposed texture descriptors, the CMLSP_LS/MM/MS still gains significant performance superiority. More significantly, it could achieve improvements of 1.54 p.p., 1.98 p.p., 2.66 p.p., and 3.98 p.p. over the accuracy of recent FbLBPACPS: 94.74%, 93.24%, 90.24%, and 82.52% for training numbers 20, 15, 10, and 5. It also outperforms the recently published CMPE by 1.39 p.p., 1.70 p.p., 2.72 p.p., and 3.77 p.p. with the same experimental conditions. In addition, in the case of (R, P) = (1, 8) and (2, 16), similar conclusions can be found in this database. The superior performance confirms the validity and efficiency of our descriptor in promoting texture classification accuracy.

Fig. 6 illustrates the classification accuracies of deep learning-based methods compared to the proposed CMLSP on the UIUC database. It is worth mentioning that the proposed CMLSP descriptor outperforms modern deep learning methods. More specifically, CMLSP achieves the best result of 96.28% on UIUC database, which is higher than FC-CNN VGGM and DeCAF by 1.78 p.p. and 2.08 p.p., respectively. In addition, it also surpasses the recent DSTNet by 2.68 p.p. Compared with the deep learning methods, the proposed CMLSP not only achieves impressive classification performance, but also doesn't require large amounts of training data and computational costs.

DISCUSSION

In this paper, we propose a CMLSP_LS/MM/MS descriptor for texture classification. Firstly, we design four 1-bit binary patterns, including LCP, LMP, LVP, and LRP, to represent local neighborhood statistical information. Secondly, a compact multi-pattern encoding strategy is adopted to combine the four binary patterns, generating a novel multi-scale local statistics pattern that efficiently captures local statistical information, particularly beneficial for complex intra-class variations. Finally, we jointly fuse MLSP, LSP, and LMP to develop a novel completed multi-scale local statistics pattern (CMLSP) for comprehensive local texture representation.

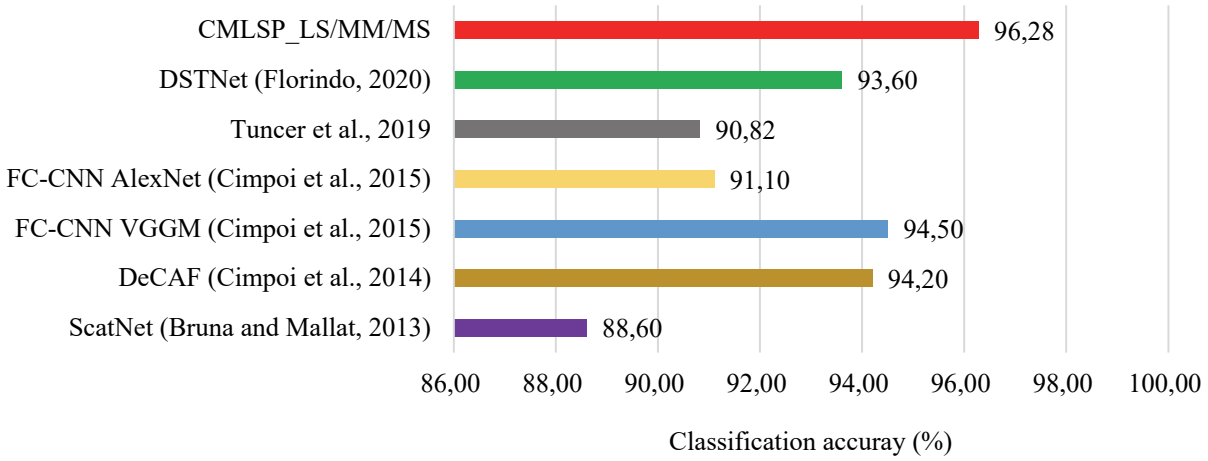

Fig. 6. *Comparison results between CMLSP and deep learning-based methods on the UIUC database.*

The performance superiority on three public texture benchmark shows that the proposed CMLSP descriptor is very informative and high-discriminative for texture classification task. Specifically, our CMLSP achieves the best results of 99.95%, 98.66%, 98.63%, 98.89%, and 96.28% on the Outex_TC10, TC12_000, TC12_001, UMD and UIUC databases respectively. It offers competitive performance and surpasses most handcrafted descriptors and deep learning-based methods. In summary, the proposed CMLSP serves as a highly discriminative and powerful descriptor for challenging texture classification tasks. Its superior performance stems from the introduction of the sub-pattern CMLSP_MS, which provides high-discriminative complementary information for texture representation. On the other hand, the joint fusion feature efficiently enhances the classification performance for challenging texture representation tasks. In the future, we aim to apply our methods to other domains such as medical image processing, plant leaf diseases analysis, and iris recognition.

ACKNOWLEDGMENTS

The paper is funded by Fujian Natural Science Foundation Project (2023J05243), Fashu Charity Foundation Donation Fund Research Special (No. MFK23003), Fujian Province Young and Middle-aged Teacher Education Research Project (JAT220312), and Minjiang University Scientific Research Promotion Fund (MJY22015).

REFERENCES

Arya R, Vimina ER (2021). Local Triangular Coded Pattern: A Texture Descriptor for Image Classification. IETE J Res (1): 1-12.

Bandzi P, Oravec M, Pavlovicova J. (2007). New Statistics for Texture Classification Based on Gabor Filters. Radioengineering 16(3): 133-7.

Banerjee P, Bhunia AK, Bhattacharyya A, Roy PP, Murala S (2018). Local Neighborhood Intensity Pattern: A new texture feature descriptor for image retrieval. Expert Syst Appl 113:100-15.

Bruna J, Mallat S (2013). Invariant scattering convolution networks. IEEE T Pattern Anal 35(8): 1872-86.

Cimpoi M, Maji S, Kokkinos I, Mohamed S, Vedaldi A (2014). Describing textures in the wild. Proceedings of CVPR 2014, Washington, DC, USA, 3606-13.

Cimpoi M, Maji S, Vedaldi, A. (2015). Deep filter banks for texture recognition and segmentation. Proceedings of CVPR 2015, Boston, MA, USA, 3828-36.

Cohen FS, Fan Z, Patel MA (1991). Classification of rotated and scaled textured images using Gaussian Markov random field models. IEEE T Pattern Anal 13(02): 192-202.

Cote M, Albu AB (2015). Robust Texture Classification by Aggregating Pixel-Based LBP Statistics. IEEE Signal Proc Let 22(11): 2102-6.

Dana KJ, Van Ginneken B, Nayar SK, Koenderink JJ, (1999). Reflectance and texture of real-world surfaces. ACM T Graphic 18(1): 1-34.

Davis LS, Johns SA, Aggarwal JK (1979). Texture analysis using generalized co-occurrence matrices. IEEE T Pattern Anal 3: 251-9.

Faust O, Acharya UR, Meiburger K, Molinari F, Koh JEW, Yeong C, Kongmebhol P, Ng K (2018). Comparative assessment of texture features for the identification of cancer in ultrasound images: A review. Biocybern Biomed Eng 38(2): 275-96.

Florindo JB, Bruno OM (2013). Texture analysis by multiresolution fractal descriptors. Expert Syst Appl 40(10): 4022-8.

Florindo JB (2020). DSTNet: Successive applications of the discrete Schroedinger transform for texture recognition. Inform Sciences 507: 356-64.

Florindo JB (2024). Fractal pooling: A new strategy for texture recognition using convolutional neural networks. Expert Syst Appl 243: 122978.

Franklin SE, (2020). Interpretation and use of geomorphometry in remote sensing: a guide and review of integrated applications. Int J Remote Sens 41(19): 7700-33.

Ganesan A, Santhanam SM (2021). Local Neighbourhood Edge Responsive Image Descriptor for Texture Classification Using Gaussian Mutated JAYA Optimization Algorithm. Arab J Sci Eng 46: 8151-70.

Guo Z, Zhang L, Zhang D (2010a). A Completed Modeling of Local Binary Pattern Operator for Texture Classification. IEEE T Image Process 19(6): 1657-63.

Guo Z, Zhang L, Zhang D. (2010b). Rotation invariant texture classification using LBP variance (LBPV) with global matching. Pattern Recogn 43(3): 706-19.

Iloanusi ON, Ezema CA (2017). A quantitative impact of fingerprint distortion on recognition performance. Lect Notes Comput Sc 26(6): 267-75.

Jain LC, Nanni L, Lumini A (2016). Local binary patterns: new variants and applications. Springer, NY: 281p.

Kim NC, So HJ (2018). Directional statistical Gabor features for texture classification. Pattern Recogn Lett 112(SEP.1): 18-26.

Kwak C, Han W (2020). Towards Size of Scene in Auditory Scene Analysis: A Systematic Review. J Audiol Otol 24(1): 1-9.

Lewicki MS, Olshausen BA, Surlykke A, Moss CF (2014). Scene analysis in the natural environment. Front Psychol 5:199.

Li Y, Xu X, Li B, Ye F, Dong Q (2018). Circular regional mean completed local binary pattern for texture classification. J Electron Imaging 27(4)

Liu L, Chen J, Fieguth P, Zhao G, Chellappa R, Pietikäinen M (2019). From BoW to CNN: Two Decades of Texture Representation for Texture Classification. Int J Comput Vision 127(1): 74-109.

Liu L, Fieguth PW, Hu D, Wei Y, Kuang G (2015). Fusing Sorted Random Projections for Robust Texture and Material Classification. IEEE T Circ Syst Vid 25(3): 482-96.

Liu L, Lao S, Fieguth PW, Guo Y, Wang X, Pietikäinen M (2016). Median Robust Extended Local Binary Pattern for Texture Classification. IEEE T Image Process 25(3): 1368-81.

Liu L, Fieguth P, Guo Y, Wang X, Pietikäinen M (2017). Local binary features for texture classification: Taxonomy and experimental study. Pattern Recogn 62: 135-60.

Liu L, Long Y, Fieguth PW, Lao S, Zhao G (2014). BRINT: Binary Rotation Invariant and Noise Tolerant Texture Classification. IEEE T Image Process 23(7): 3071-84.

Liu L, Zhao L, Long Y, Kuang G, Fieguth P (2012). Extended local binary patterns for texture classification. Image Vision Comput 30(2): 86-99.

Manjunath BS, Ohm JR, Vinod VV, Yamada A (2001). Color and texture descriptors. IEEE T Circ Syst Vid 11(6): 703-15.

Mehta R, Egiazarian K (2016). Dominant Rotated Local Binary Patterns (DRLBP) for texture classification. Pattern Recogn Lett 71(Feb.1): 16-22.

Nguyen TP, Vu NS, Manzanera A (2016). Statistical binary patterns for rotational invariant texture classification. Neurocomputing 173(JAN.15PT.3): 1565-77.

Nguyen VD, Nguyen D, Nguyen T, Dinh VQ, Jeon J (2014). Support Local Pattern and Its Application to Disparity Improvement and Texture Classification. IEEE T Circ Syst Vid 24(2): 263-76.

Ojala T, Pietikainen M, Maenpaa T (2002a). Multiresolution gray-scale and rotation invariant texture classification with local binary patterns. IEEE T Pattern Anal 24(7): 971-87.

jala T, Maenpaa T, Pietikainen M, Viertola J, Kyllonen J, Huovinen S (2002b). Outex - new framework for empirical evaluation of texture analysis algorithms. Proceedings of ICPR 2002, Quebec City, QC, Canada, 701-6.

Pan Z, Fan H, Zhang L (2015). Texture Classification Using Local Pattern Based on Vector Quantization. IEEE T Image Process 24(12): 5379-88.

Pan Z, Hu S, Wu X, Wang P (2021). Adaptive center pixel selection strategy to Local Binary Pattern for texture classification. Expert Syst Appl 180(4): 115123.

Pan Z, Li Z, Fan H, Wu X (2017). Feature based local binary pattern for rotation invariant texture classification. Expert Syst Appl 88: 238-48.

Pan Z, Wu X, Li Z (2019). Central pixel selection strategy based on local gray-value distribution by using gradient information to enhance LBP for texture classification. Expert Syst Appl 120: 319-34.

Patino JE, Duque JC (2013). A review of regional science applications of satellite remote sensing in urban settings. Comput Environ Urban 37(1): 1-17.

Pothos, V. K., Theoharatos, C., Zygouris, E., *et al.* (2008). Distributional-based texture classification using non-parametric statistics. Pattern Anal Appl 11(2): 117-29.

Qi X, Zhao G, Shen L, Li Q, Pietikäinen M (2016). LOAD: Local Orientation Adaptive Descriptor for Texture and Material Classification. Neurocomputing 184:28-35.

Shakoor MH, Boostani R (2017). Extended Mapping Local Binary Pattern Operator for Texture Classification. Int J Pattern Recogn 31(6): 1-22.

Silva PM, Florindo JB (2019). A statistical descriptor for texture images based on the box counting fractal dimension. Physica A 528(15): 121469.

Song T, Feng J, Wang S, Xie Y (2020). Spatially weighted order binary pattern for color texture classification. Expert Syst Appl 147: 113167.

Song K, Yan Y, Zhao Y, Liu C (2015). Adjacent evaluation of local binary pattern for texture classification. J Vis Commun Image R 33: 323-39.

Tan X, Triggs B (2010). Enhanced Local Texture Feature Sets for Face Recognition Under Difficult Lighting Conditions. IEEE T Image Process 19(6):1635-50.

Tuncer T, Dogan S, & Ertam F (2019). A novel neural network-based image descriptor for texture classification. Physica A, 526: 120955.

Unser M (1995). Texture classification and segmentation using wavelet frames. IEEE T Image Process 4(11), 1549-60.

Van der Meer F (2012). Remote-sensing image analysis and geostatistics. Int J Remote Sens 33(18): 5644-76.

Verma M, Raman B (2018). Local neighborhood difference pattern: A new feature descriptor for natural and texture image retrieval. Multimed Tools Appl 77(10): 11843-66.

Varma M, Zisserman,A (2005). A statistical approach to texture classification from single images. Int J Comput Vision 62(1–2): 61–81.

Wang K, Bichot C-E, Li Y, Li B (2017). Local binary circumferential and radial derivative pattern for texture classification. Pattern Recogn 67: 213-29.

Wang T, Dong Y, Yang C, Wang L, Liang L, Zheng L, Pu J (2018). Jumping and Refined Local Pattern for Texture Classification. IEEE Access, 6: 64416-25.

Wang S, Han K, Jin J (2019). Review of image low-level feature extraction methods for content-based image retrieval. Sensor Rev 39(6): 783-809.

Xu Y, Ji H, Fermuller C (2006). A Projective Invariant for Textures. Proceedings of CVPR 2006, New York, NY, USA, 1932-9.

Xu X, Li Y, Wu QJ (2020a). A Multiscale Hierarchical Threshold-Based Completed Local Entropy Binary Pattern for Texture Classification. Cogn Comput 12(1): 224-37.

Xu X, Li Y, Wu QJ (2020b). A completed local shrinkage pattern for texture classification. Appl Soft Comput 97: 106830.

Xu X, Li Y, Wu QJ (2021). A compact multi-pattern encoding descriptor for texture classification. Digit Signal Process 114(2): 103081.

Yu H, Yang W, Xia G-S, Liu G (2016). A color-texture-structure descriptor for high-resolution satellite image classification. Remote Sens-Basel 8(3): 259.

Zhang W, Zhang W, Liu K, Gu J (2017a). A Feature Descriptor Based on Local Normalized Difference for Real-World Texture Classification. IEEE T Multimedia 20(4): 880-8.

Zhang Z, Liu S, Mei X, Xiao B, Zheng L (2017b). Learning completed discriminative local features for texture classification. Pattern Recogn 67: 263-75.

Zhao Y, Huang DS, Jia W (2012). Completed Local Binary Count for Rotation Invariant Texture Classification. IEEE T Image Process 21(10): 4492-7.

Zhao Y, Wang R-G, Wang W-M, Gao W (2016). Local Quantization Code Histogram for Texture Classification. Neurocomputing 207(26): 354-64.

Zhao Y, Jia W, Hu R-X, Min H (2013). Completed robust local binary pattern for texture classification. Neurocomputing 106(15): 68-76.